Journal of Applied Polymer Science

Synthesis and Electrochemical Properties of Graphene Oxide/Nanosulfur/Polypyrrole Ternary Nanocomposite Hydrogel for Supercapacitors

Chunnian Chen, Xuwang Fu, Ting Ma, Wei Fan, Zhongbing Wang, Shiding Miao
Anhui Key Laboratory of Controllable Chemistry Reaction & Material Chemical Engineering, Hefei University of Technology, Hefei, Anhui 230009, People's Republic of China
Correspondence to: C. Chen (E-mail: chencn@ustc.edu)

ABSTRACT: A method for synthesizing Graphene oxide (GO)/nano-sulfur/polypyrrole (PPy) ternary nanocomposite hydrogel is depicted. The higher surface area of GO, PPy porous structure and their excellent conductivity are utilized, and the GO hydrogel can be made easily. The products are characterized by field-emission scanning electron microscopy (FESEM), X-ray diffraction (XRD), Fourier transform infrared (FTIR) spectra, and electrochemical workstation. The results demonstrated that GO/nano-S/PPy ternary nanocomposite hydrogel is successfully synthesized. The electrochemical properties are investigated by cyclic voltammetry, galvanostatic charge/discharge measurements, and cycling life in a three-electrode system in 1*M* Li_2SO_4 electrolyte solution. The GO/nano-S/PPy ternary nanocomposite hydrogel exhibit a high specific capacitance of 892.5 F g^{-1} at scan rates of 5 mV s^{-1} and the capacitance retain about 81.2% (594.8 F g^{-1}) of initial capacitance (732.5 F g^{-1}) after 500 cycles at a current density of 1 A g^{-1}. © 2014 Wiley Periodicals, Inc. J. Appl. Polym. Sci. **2014**, *131*, 40814.

KEYWORDS: conducting polymers; nanotubes; graphene and fullerenes; gels; electrochemistry; composites

Received 12 January 2014; accepted 3 April 2014
DOI: 10.1002/app.40814

INTRODUCTION

Supercapacitors, known as electrochemical capacitor, attracted considerable attention over past decades, owing to its high energy density, long cycle life, short charge/discharge time and better environmental friendliness.[1] As the materials of electrodes in supercapacitors, three potential candidates were considered: carbon materials, conducting polymers, and inorganic oxides.[2,3] As unique carbon materials, graphene is taking into consideration of its tensile strength, low density, high elasticity and tremendously large surface area.[4–6] Hence, graphene is widely used in electrochemical supercapacitor fields. GO, which possesses many oxygen-containing groups on its basal planes and edges, is one of the most important derivatives of graphene.[7] Conducting polymers, such as polyaniline,[8] polythiophene,[9] and PPy,[10,11] have been used as electrode materials for supercapacitor due to their morphology, high electrical conductivity, and good electrochemical stability. Compared with other electrode materials, the special performance of sulfur(S) is owing to its low cost, high theoretical capacity of 1672 mA h g^{-1}, abundance and environmental friendliness.[12] However, it is generally recognized that the challenge associated with the poor electronic conductivity (5×10^{-30} S cm^{-1} at 25°C) and the poor cycle life.[13] So, the carbon materials and conducting polymers have been taken into account to improve their electronic conductivity and cycle life.[14–17] Thus, GO/nano-S/PPy ternary nanocomposite was synthesized to increase the electric conductivity and cycling stability of sulfur.[12]

Recently, there has been a widespread using over the flexible electronics in our daily life and the high-performance flexible solid-state supercapacitors are also an increasing demand for power supply.[18–23] The two-dimensional (2D) graphene is taking into consideration of building blocks to make ultralight yet strong and compressible materials. Graphene gels consist of interconnected porous frameworks with large specific surface areas, convenient electrolyte diffusion, and electron transport. They have been used as supercapacitors materials because its large capacitances, excellent electronic conductivity, easy separation, simple assemble, and cycling stability.[24–26] In addition, the hydrogel has been used as binder-free electrode materials.[27] Oxalic acid was taken into consideration as linked to form hydrogel owing to carboxyl group from oxalic acid can be combine with hydroxyl group from GO. Herein, the GO/nano-S/PPy ternary nanocomposite hydrogel was obtained with a high electrochemical performance.

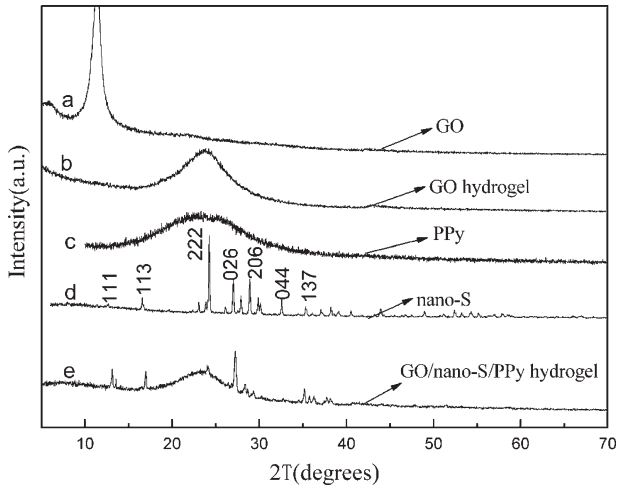

Figure 1. XRD pattern of (a) GO, (b) GO hydrogel, (c) PPy, (d) nano-S, and (e) GO/nano-S/PPy nanocomposite hydrogel.

EXPERIMENTAL

Synthesis of GO/Nano-S/PPy Composite

GO was prepared from graphite powder using a modified Hummers method.[28] $Na_2S_2O_3{\cdot}5H_2O$ (0.2 mmol) was dispersed into 50 mL GO dispersion (2.5 mg mL^{-1}). After addition of 0.8 mL HCl (10*M*), this solution ultrasonic stirred for 1 h. And then, the GO/nano-S was washed by deionized water and separated by centrifugation.

To make GO/nano-S/PPy composite, as-prepared GO/nano-S was redispersed into 50 mL aqueous solution. And then, L-lysine (0.2 mmol), pyrrole monomer (25 μL), and $(NH_4)_2S_2O_8$ (0.2 mmol) were added under ultrasonic agitation.[29] After reaction for 4 h, the mixture was washed by deionized water and separated by centrifugation and ultrasonic dispersed into 100 mL aqueous solution to obtain the GO/nano-S/PPy composite suspension.

Synthesis of GO/Nano-S/PPy Ternary Nanocomposite Hydrogel

In a topical process, GO/nano-S/PPy suspension (6.0 mL) was mixed uniformly with oxalic acid (0.02 g). The mixed solution sealed in a glass vial and take hydrothermal treatment for 24 h at 95°C for synthesis of GO/nano-S/PPy ternary nanocomposite hydrogel.

Electrochemical Characterization

Electrochemical performance were characterized by cyclic voltammetry (CV) and galvanostatic charge/discharge on a CHI660 electrochemical workstation system. The electrolyte was 1*M* Li_2SO_4 solution and the three-electrode system was equipped with a platinum foil counter electrode and a saturated calomel reference electrode.

The working electrodes were prepared by 100 wt % electroactive materials dissolved in *N*-methyl pyrrolidone to form slurry. The slurry was uniformly spread coated onto a nickel foam current collector.

Based on the CV and charge/discharge curve, the specific capacitance can be calculated according to the following equation $C = (\int I\mathrm{d}v)/(v\mathrm{m}\Delta V)$ and $C = (I\Delta t)/(\mathrm{m}\,\Delta V)$, respectively, where I is the constant discharge current (A), v is the potential (V), ΔV is voltage drop during discharge process (V), v is the potential scan rate (mV s^{-1}), m is the mass of electroactive material (g), and $\triangle t$ is the discharge time (s).

RESULTS AND DISCUSSION

XRD Analysis

XRD patterns of GO, GO hydrogel, PPy, nano-S, and GO/nano-S/PPy nanocomposite hydrogel were shown in Figure 1. The typical diffraction peak of GO appears at around 11°, as shown in Figure 1(a).[30] The pattern of GO hydrogel diffraction peak at around 24° and the broadband appears at 20–28° appears, as shown in Figure 1(b),[31,32] and it could be seen that the peaks of GO were disappeared because the order structure of GO sheets was destroyed when the GO was gelatination.[33] The broad peak located in the range of 18–30° and centered at $2\theta = 24°$, which was the characteristic peak of PPy,[2,34] as shown in Figure 1(c). All the diffraction peaks of pure S shown in Figure 1(d) are readily indexed to S (JCPDS: 08–0247) with orthorhombic phase, indicating high purity phase of the as-synthesized S products. The diffraction peaks at $2\theta = 12.5°$, 16.5°, 24.2°, 26.9°, 28.8°, 32.6°, and 35.3° corresponds to (111), (113), (222), (026), (206), (044), and (137) crystal planes, respectively. The XRD pattern of GO/nano-S/PPy nanocomposite hydrogel was shown in Figure 1(e), the broadband peak located in the range of 18–26° that was the characteristic peak of GO hydrogel and PPy. However, the nanocomposite hydrogel does not show the peaks of S in XRD spectra clearly, it could be indication of low content compared with GO and PPy.

Morphology of the Composite

Photographs of the dispersion solution and hydrogel of GO/nano-S/PPy nanocomposite were shown in Figure 2(a). FESEM image of GO/S was shown in Figure 2(b), it can be more clearly seen that the nano-S particles deposited on the GO sheets. The surface morphology of the GO/nano-S/PPy ternary nanocomposite hydrogel was seen in the FESEM Figure 2(c). The size of nano-S particles is very difficult to be controlled owing to the complexity of its nucleus and growth progress affected by many no-line factors. So, the size of nano-S particle shown in Figure 2(b) is a little difference than that of nano-S particle shown in Figure 2(c). The content of PPy is so low that Figure 2(b,c) has little difference as FESEM observed. The energy-dispersive spectrometer (EDS) pattern was shown in Figure 2(d). In Area 5, the possible elements were measure by EDS method. As a result, S and nitrogen elements content indicated the existence of S and PPy, respectively. The sodium and chlorine elements existed because the nano-S preparation used the $Na_2S_2O_3{\cdot}5H_2O$ and HCl. It is observed through the Figure 2(b–d) that the sulfur particles deposited on the GO sheets and coated by PPy.

FTIR Spectra Analysis

FTIR spectral analysis was performed to confirm the chemical structure of the GO/nano-S/PPy nanocomposite hydrogel. The FTIR spectra of GO, PPy, and GO/nano-S/PPy nanocomposite hydrogel were shown in Figure 3. For pure GO, observed broad absorption band at 3389 cm^{-1} is the stretching vibration absorption of hydroxyl groups in water molecules. The bending

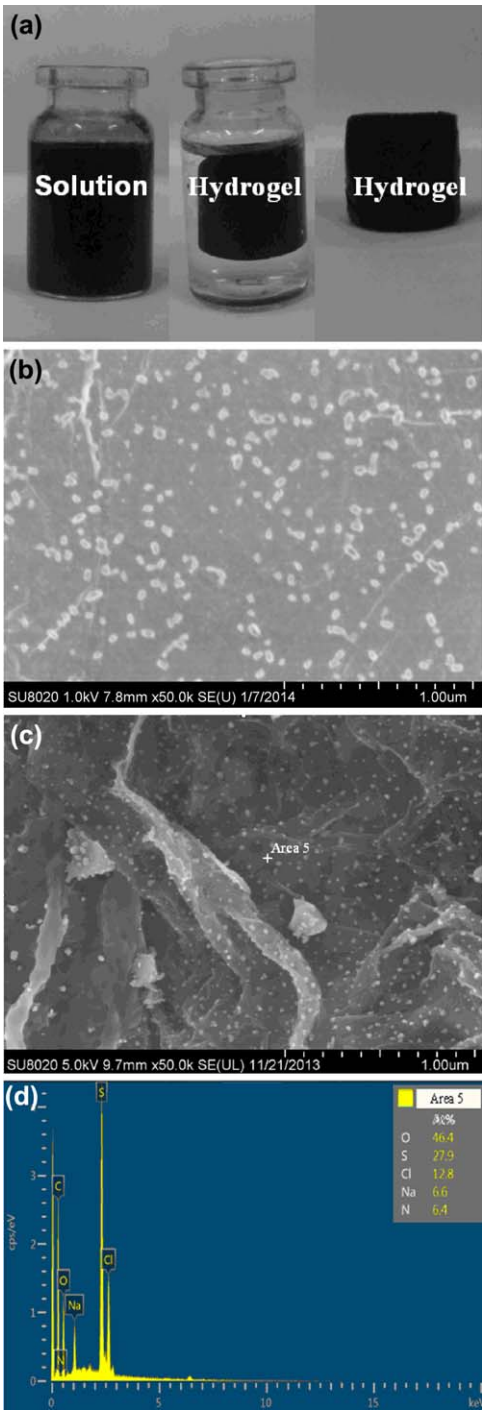

Figure 2. (a) Photographs an aqueous dispersion solution and hydrogel of GO/nano-S/PPy nanocomposite. (b) and (c) FESEM image of GO/S and GO/S/PPy nanocomposite hydrogel. (d) EDS pattern of GO/S/PPy nanocomposite hydrogel. [Color figure can be viewed in the online issue, which is available at wileyonlinelibrary.com.]

vibration from O–H groups is detected at 1406 cm^{-1}. The absorption peaks located at 1729, 1624, 1222, and 1055 cm^{-1} corresponds to the C═O, C═C, and C—O in COH or COC functional groups stretching vibration of the GO sheets, respectively.[35] For pure PPy polymer, the broad band at 3127 cm^{-1} is

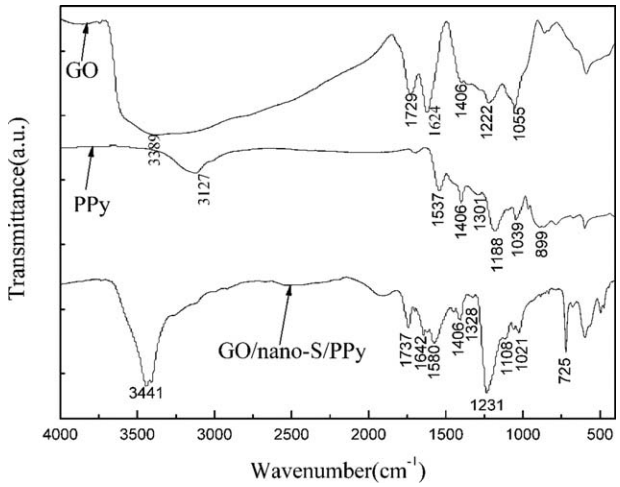

Figure 3. FTIR spectra of GO, PPy and GO/nano-S/PPy nanocomposite hydrogel.

attributed to the N–H stretching vibration. The peaks at 1537 and 1406 cm^{-1} could be associated with C—N and C—C asymmetric and symmetric ringstretching.[2] The broadband at 1301, 1188, 1039, and 899 cm^{-1} are ascribed to the C-H in-plane deformation vibrations, C-N stretching vibrations, N-H in-plane deformation vibrations, and C-H out-of-plane vibration, respectively.[36] Compared to FTIR spectra of individual GO and PPy, all the characteristic peaks have appeared in the spectra of GO/PPy/S nanocomposite hydrogel, such as 3441, 1737, 1642, 1580, 1406, 1328, 1108, 1021, and 775 cm^{-1}, implies that PPy chains have been integrated with GO to form the GO/S/PPy composite.

Raman Spectra Analysis

Raman spectra is an effective tool for characterizing carbonaceous materials, particularly for distinguishing ordered and disordered crystal structures of carbon. The Raman spectra for the GO hydrogel and GO/nano-S/PPy ternary nanocomposite hydrogel were shown in Figure 4. For GO hydrogel, the D band (1357 cm^{-1}) and G band (1593 cm^{-1}), were essentially identical to the characteristic peaks of GO.[37] The D band

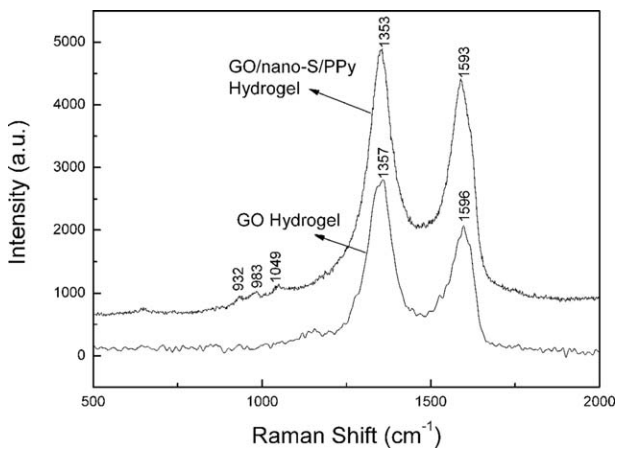

Figure 4. Raman spectra of GO hydrogel and GO/nano-S/PPy ternary nanocomposite hydrogel.

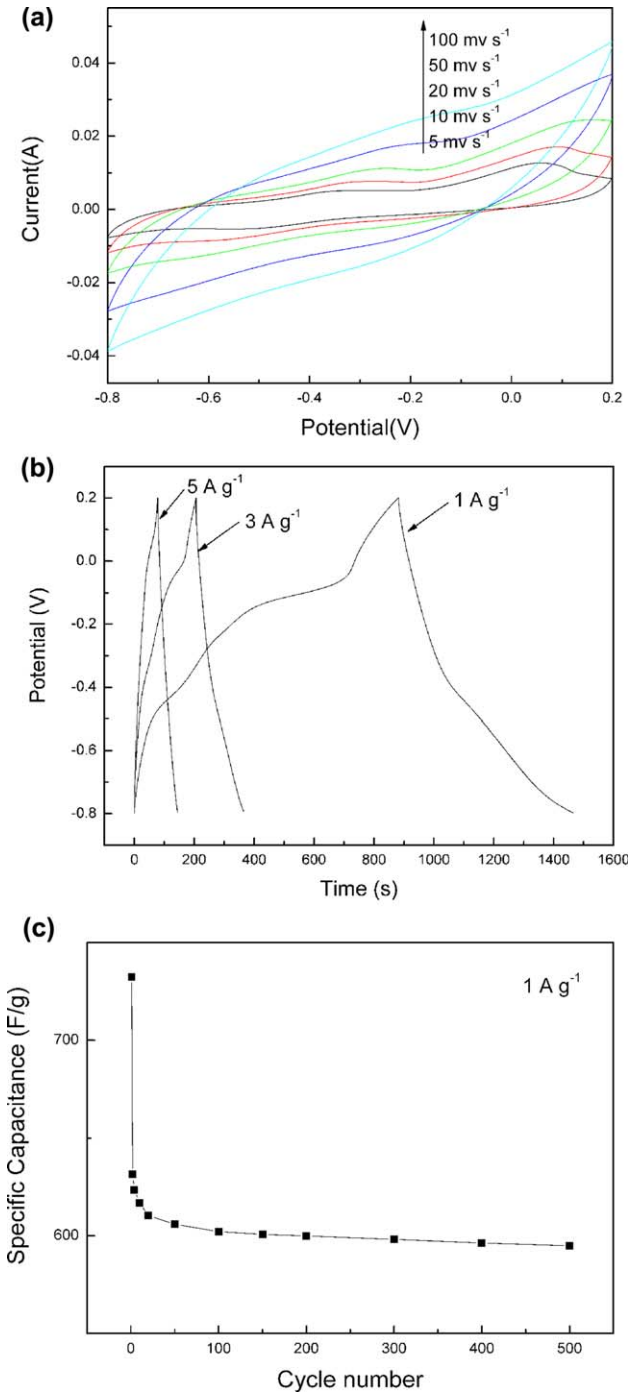

Figure 5. (a) CV curves of the GO/nano-S/PPy ternary nanocomposite hydrogel at different scan rates of 5, 10, 20, 50, and 100 mV s^{-1}. (b) Galvanostatic charge/discharge curves of GO/nano-S/PPy ternary nanocomposite hydrogel at current densities of 5, 3, and 1 A g^{-1}. (c) Cycling life of GO/nano-S/PPy ternary nanocomposite hydrogel at a current density of 1 A g^{-1}. [Color figure can be viewed in the online issue, which is available at wileyonlinelibrary.com.]

corresponded to breathing modes of aromatic rings and the G band represents the in-plane bond-stretching motion of the pairs of C sp^2 atoms.[38] The disorder of GO was increased due to the hydrogel formed. So, the higher intensity of D band was existed. Compared with GO hydrogel, the characteristic peaks D band (1353 cm^{-1}) and G band (1593 cm^{-1}) have also appeared of GO/nano-S/PPy nanocomposite hydrogel. The peaks at 1049, 983, and 932 cm^{-1} have been associated with the quinonoid polaronic and quinonoid bipolaronic structure, revealing the presence of the doped PPy structure.[36] Combined with XRD, FESEM, EDS, and FTIR spectra, GO/nano-S/PPy ternary nanocomposite hydrogel was successful synthesized.

Electrochemical Performance

To explore the electrochemical performance of the GO/nano-S/PPy ternary nanocomposite hydrogel, CV, galvanostatic charge/discharge measurements and cycling life were tested in a three-electrode system in 1*M* Li_2SO_4 electrolyte solution. The CV tests at different scan rates ranged 5–100 mV s^{-1} were depicted in Figure 5(a). All CV curves with a distortion even have a secondary oxidation peak at a low scan rate due to the nano-S were continue oxidized to the higher-order polysulphides (S_n^{2-}, $n \geqq 4$).[10,12] High absorption ability of PPy to sulfur can keep polysulphides form dissolving in the liquid electrolyte.[39] It is found that the specific capacitance of GO/nano-S/PPy ternary nanocomposite hydrogel supercapacitor were 892.5, 636.9, 420.0, 248.3, and 163.1 F g^{-1} at scan rates of 5, 10, 20, 50, and 100 mV s^{-1}, respectively. The specific capacitances were 710, 236, and 52 F g^{-1} of GO/PPy, PPy, and GO at scan 2 m V^{-1}, respectively.[7] Thus, the GO/nano-S/PPy ternary nanocomosite hydrogel exhibits the larger specific capacitance owing the sulfur existed. The galvanostatic charge/discharge curves at different current density were shown in Figure 5(b). The special capacitances were 732.5, 547.2, and 332.5 F g^{-1} at current density of 1, 3, and 5 A g^{-1}, respectively. Furthermore, the cycling life of GO/nano-S/PPy ternary nanocomposite hydrogel was investigated in the range of −0.8 to 0.2 V at a current density of 1 A g^{-1}. As shown in Figure 5(c), the capacitance retained about 81.2% (594.8 F g^{-1}) of initial capacitance after 500 cycles. Meanwhile, the GO/nano-S/PPy ternary nanocomposite hydrogel has excellent conductivity (0.018 S cm^{-1} at 25°C) by Electrical Conductivity Meter measured. Compared with other sulfur electrode materials, the GO/nano-S/PPy ternary nanocomosite hydrogel electrode materials exhibit high special capacitances, excellent cycling life and excellent conductivity, which can be attributed to the synergistic effect of each component. Graphene oxide provided high area for S deposition to avoid the S gather. Meanwhile, the GO and PPy have excellent conductivity which favors for electronic conductive channels. The PPy porous structure can adjust the volume conversion during cycling.

CONCLUSIONS

In summary, the GO/nano-S/PPy ternary nanocomposite hydrogel was successfully synthesized and characterized by XRD, FESEM, Photographs, FTIR, Raman, and Electrochemical. In the process of experiment, S was deposited on the high surface area of GO and then GO/nano-S was coated by porous structure PPy, which favors for electronic conductive channels and adjust the volume conversion during galvanostatic charge/discharge. Meanwhile, the GO hydrogel was formed easily and can be used as binder-free electrode materials with environmental friendliness. Supercapacitors based on the GO/nano-S/PPy

ternary nanocomposite hydrogel exhibited high specific capacitance, excellent cycling life and excellent conductivity. The CV showed specific capacitance as high as 892.5 F g^{-1} at scan rate of 5 mV s^{-1}. The specific capacitance retained 81.2% (594.8 F g^{-1}) of initial capacitance (732.5 F g^{-1}) after 500 cycles at a current density of 1 A g^{-1}. This kind of ternary nanocomposite hydrogel is a promising candidate for high performance of supercapacitor applications.

ACKNOWLEDGMENTS

Gratefully acknowledge financial support from the Hefei University of Technology, school-enterprise cooperation projects production (106-433168) of China.

REFERENCES

1. Yan, J.; Fan, Z. J.; Wei, T.; Zhang, M. L. *J. Mater. Sci. Mater. Electron.* **2010**, *21*, 619.
2. Zhang, A. Q.; Xiao, Y. H.; Lu, L. Z.; Wang, L. Z.; Li, F. *J. Appl. Polym. Sci.* **2012**, *128*, 1327.
3. Qian, T.; Yu, C. F.; Wu, S. S.; Shen, J. *J. Mater. Chem. A* **2013**, *1*, 6539.
4. Sun, Y. Q.; Wu, Q. Q.; Shi, G. Q. *Energy Environ. Sci.* **2011**, *4*, 1113.
5. Huang, Y.; Liang, J. J.; Chen, Y. S. *Small* **2012**, *8*, 1805.
6. Zhai, Y. P.; Dou, Y. Q.; Zhao, D. Y.; Fulvio, P. F.; Mayes, R. T.; Dai, S. *Adv. Mater.* **2011**, *23*, 4828.
7. Li, J.; Xie, H. Q.; Li, Y. *J. Power Sources* **2013**, *241*, 388.
8. Li, G. C.; Li, G. R.; Ye, S. H.; Gao, X. P. *Adv. Energy Mater.* **2012**, *2*, 1238.
9. Wu, F.; Wu, S.; Chen, R.; Chen, J.; Chen, S. *Electrochem. Solid-State Lett.* **2010**, *13*, A29.
10. Liang, X.; Liu, Y.; Wen, Z. Y.; Huang, L. Z.; Wang, X. Y.; Zhang, H. *J. Power Sources* **2011**, *196*, 6951.
11. Zhang, Y.; Bakenov, Z.; Zhao, Y.; Konarov, A.; Doan, T. N. L.; Malik, M.; Paron, T.; Chen, P. *J. Power Sources* **2012**, *208*, 1.
12. Zhang, Y. G.; Zhao, Y.; Konarow, A.; Gosselink, D.; Soboleski, H. G.; Chen, P. *J. Power Sources* **2013**, *241*, 517.
13. Seh, Z. W.; Li, W. Y.; Cha, J. J.; Zheng, G. G.; Yang, Y.; McDowell, M. T.; Hsu, P. C.; Cui, Y. *Nat. Commun.* **2013**, *4*, 1331.
14. Sahoo, S.; Bhattacharya, P.; Hatui, G.; Ghosh, D.; Das, C. K. *J. Appl. Polym. Sci.* **2012**, *128*, 1476.
15. Lim, Y. S.; Tan, Y. P.; Lim, H. N.; Tan, W. T.; Mahnaz, M. A.; Talib, Z. A.; Huang, N. M.; Kassim, A.; Yarmo, M. A. *J. Appl. Polym. Sci.* **2012**, *128*, 224.
16. Lin, J. X.; Zheng, Y. Y.; Du, Q. F.; He, M. P.; Deng, Z. W. *NANO* **2013**, *8*, 1350004-1.
17. Qian, T.; Wu, S. S.; Shen, J. *Chem. Commun.* **2013**, *49*, 4610.
18. Cao, Q.; Kim, H. S.; Pimparkar, N.; Kulkarni, J. P.; Wang, C.; Shim, M.; Roy, K.; Alam, M. A.; Rogers, J. A. *Nature* **2008**, *454*, 495.
19. Nishide, H.; Oyaizu, K. *Science* **2008**, *319*, 737.
20. Meng, C. Z.; Liu, C. H.; Chen, L. Z.; Hu, C. H.; Fan, S. S. *Nano Lett.* **2010**, *10*, 4025.
21. Choi, B. G.; Hong, J.; Hong, W. H.; Hammond, P. T.; Park, H. *ACS Nano* **2011**, *5*, 7205.
22. Xu, Y. X.; Lin, Z. Y.; Huang, X. Q.; Liu, Y.; Huang, Y.; Duan, X. F. *ACS Nano* **2013**, *7*, 4042.
23. Xu, Y. X.; Huang, X. Q.; Lin, Z. Y.; Zhong, X.; Huang, Y.; Duan, X. F. *Nano Res.* **2013**, *6*, 65.
24. Zhao, Y.; Liu, J.; Chen, H. H.; Hu, C. G.; Jiang, C. C.; Jiang, L.; Cao, A. Y.; Qu, L. T. *Adv. Mater.* **2013**, *25*, 591.
25. Zhang, L.; Zhang, F.; Yang, X.; Long, G. K.; Wu, Y. P.; Zhang, T. F.; Leng, K.; Huang, Y.; Ma, Y. F.; Yu, A.; Chen, Y. S. *Sci. Rep.* **2013**, *3*, 1408.
26. Zhang, L.; Yang, X.; Zhang, F.; Long, G. K.; Zhang, T. F.; Leng, K.; Zhang, Y. W.; Huang, Y.; Ma, Y. F.; Zhang, M. T.; Chen, Y. S. *J. Am. Chem. Soc.* **2013**, *135*, 5921.
27. Xu, Y. X.; Lin, Z. Y.; Huang, Q.; Wang, Y.; Duan, X. F. *Adv. Mater.* **2013**, *25*, 5779.
28. Hummers, W. S.; Offeman, R. E. *J. Am. Chem. Soc.* **1958**, *80*, 1339-9.
29. Camacho, A. R.; Franco, L. E. N. *Rev. Mex. Fis. S* **2013**, *59*, 147.
30. Zhu, Y. W.; Murali, S.; Stoller, M. D.; Velamakanni, A.; Piner, R. D.; Ruoff, R. S. *Carbon* **2010**, *48*, 2118.
31. Luan, V. H.; Tien, H. N.; Hoa, L. T.; Hien, N. T. M.; Oh, E. S.; Chuang, J. S. *J. Mater. Chem. A* **2013**, *1*, 208.
32. Cong, H. P.; Wang, P.; Yu, S. H. *Communications* **2014**, *10*, 448.
33. Hu, H.; Zhao, Z. B.; Wan, W. B.; Gogotsi, Y.; Qiu, J. S. *Adv. Mater.* **2013**, *25*, 2219.
34. Das, D.; Nath, B. C.; Phukon, P.; Saikia, B. J.; Kamrupi, I. R.; Dolui, S. K. *Materrals Chemisrty and Physics.* **2013**, *142*, 61.
35. Singh, V. K.; Patra, M. K. *New Carbon Materials.* **2009**, *24*, 147.
36. Yang, S. D.; Shen, C. M.; Liang, Y. Y.; Tong, H.; He, W.; Shi, X.Z.; Zhang, X. G.; Gao, H. J. *Nanoscale.* **2011**, *3*, 3277.
37. Zeng, P.; Zhang, Q. G.; Zhang, X. G.; Peng, T. Y. *J. Alloys Compd.* **2012**, *516*, 85.
38. Chen, L.; Xu, Z. W.; Li, J. L.; Li, Y. L.; Shan, M. J.; Wang, C. H.; Wang, Z.; Guo, Q. W.; Liu, L. S.; Chen, G. W.; Qian., X. M. *J. Mater. Chem.* **2012**, *22*, 13460.
39. Wang, W.; Li, G. C.; Wang, Q.; Li, G. R.; Ye, S. H.; Gao, X. P. *J. Electrochem. Soc.* **2013**, *160*, A805.